Elsevier Editorial System(tm) for
International Journal of Hydrogen Energy
Manuscript Draft

Manuscript Number:

Title: Synthesis and characterization of a Mg-Ni-RE alloy for hydrogen storage

Article Type: Full Length Article

Section/Category: Hydrides / Storage / Capacitors

Keywords: Hydrogen storage, Mg base alloy, Dynamic absorption/desorption conditions, Dehydrogenation kinetics

Corresponding Author: Dr. Alessandro Dell'Era,

Corresponding Author's Institution:

First Author: Alessandro Dell'Era

Order of Authors: Alessandro Dell'Era; Mauro Pasquali; Stefano Vecchio Ciprioti; Carla Lupi; Andrea Brotzu; Francesco Mura; Riccardo Tuffi

Abstract: The synthesis and characterization of a Mg-Ni alloy having La and Ce as catalysts, have been performed. The alloy behavior was studied at given fixed temperature and pressure during hydrogen absorption/desorption tests. The La and Ce addition was carried out starting from a commercial alloy, named "Firesteel". The alloy synthesized has the following formula Mg68Ni26M5X,where X represents Si and Fe impurities and M stands for the mixture of rare earths metals. The alloy has been prepared by a melting process in an induction furnace equipped with a centrifugal casting system and then grinded, by both hydraulic press and ball milling. The alloy has been characterized by SEM, BET, XRD, DSC-TGA analysis and by a mass flow measurement apparatus. The experiments on alloy sample showed that, after activation, hydrogenation occurs at 300 °C in three stages at three different pressures: 3, 4 and 7 atm, involving respectively 0.15%, 0.4% and 2.2% of hydrogen absorbed. Reversible hydride dehydrogenation, inside the mass flow measurement apparatus, requires a working temperature of 350 °C to obtain hydrogen desorption of about 2.7 % at a remarkable reaction rate.

STATEMENT LETTER OF THE ARTICLE:

"*Synthesis and characterization of a Mg-Ni-RE alloy for hydrogen storage"*

A. Dell'Era, M. Pasquali, S. Vecchio Ciprioti, A. Brotzu, C. Lupi, F. Mura, R. Tuffi

Dear Editor

It is stated, in this letter, that the submitted paper has not been published previously, is not under consideration for publication elsewhere, and if accepted will not be published elsewhere in the same form, in English or in any other language, without the written consent of the publisher. The authors have no commercial associations or sources of support that might pose a conflict of interest. All authors have made substantive contributions to the study.

Sincerely

Dr. Alessandro Dell'Era

***Highlights (for review)**

- Mg-Ni based alloy synthesis for hydrogen storage application has been performed
- The alloy has been produced by adding “Firesteel”, that contains Metal Rare Earths
- Characterization by SEM, BET, XRD, DSC-TG analyses and by mass flow type apparatus
- Reversible hydrogen desorption of about 2.7 % with good reaction rate was obtained
- The temperature desorption presenting a faster kinetic is about 350 ° C

Synthesis and characterization of a Mg-Ni-RE alloy for hydrogen storage

A. Dell'Era[a,b], M. Pasquali[a], S. Vecchio Ciprioti[a], C. Lupi[c], A. Brotzu[c], F. Mura[a], R. Tuffi[d]

[a] Department S.B.A.I., Sapienza University of Rome, Via del Castro Laurenziano 7, I-00161 Roma, Italy Department
alessandro.dellera70@gmail.com
[b] CNR, Istituto di Struttura della Materia, Via Salaria, km. 29.300, c.p. 10, I-00016 Monterotondo Scalo, Roma, Italy
[c] Department I.C.M.A., Sapienza University of Rome, Via Eudossiana 18, I-00184 Roma, Italy
[d] ENEA - Casaccia Research Center, Via Anguillarese 301, 00123 Roma, Italy

Abstract

The synthesis and characterization of a Mg-Ni alloy having La and Ce as catalysts, have been performed. The alloy behavior was studied at given fixed temperature and pressure during hydrogen absorption/desorption tests. The La and Ce addition was carried out starting from a commercial alloy, named "Firesteel". The alloy synthesized has the following formula $Mg_{68}Ni_{26}M_5X$, where X represents Si and Fe impurities and M stands for the mixture of rare earths metals. The alloy has been prepared by a melting process in an induction furnace equipped with a centrifugal casting system and then grinded, by both hydraulic press and ball milling. The alloy has been characterized by SEM, BET, XRD, DSC-TGA analysis and by a mass flow measurement apparatus. The experiments on alloy sample showed that, after activation, hydrogenation occurs at 300 °C in three stages at three different pressures: 3, 4 and 7 atm, involving respectively 0.15%, 0.4% and 2.2% of hydrogen absorbed. Reversible hydride dehydrogenation, inside the mass flow measurement apparatus, requires a working temperature of 350 °C to obtain hydrogen desorption of about 2.7 % at a remarkable reaction rate.

Keywords: Hydrogen storage, Mg base alloy, Dynamic absorption/desorption conditions, Dehydrogenation kinetics

Introduction

The design of storage units using metal hydrides has been the subject of several studies in the recent years [1-13] and presents many complexities because of a wide range of temperature and pressure. Mg-based alloy should be ideal candidates for hydrogen storage [14-23], however, the Mg-based materials have rather high dissociation temperatures, slow reaction rates and achieve their activation very hardly, thus making them virtually useless in many practical applications. Among these alloys, also Mg_2Ni cannot absorb hydrogen under normal conditions (i.e. room temperature and atmospheric pressure), and the best conditions for hydrogenation seem to be achieved at temperature range from 250–350 °C with hydrogen pressure of 15–50 atm. In addition it needs to be activated before hydrogenation. Several papers were published in the past regarding the upgrade of hydrogenation properties for Mg_2NiH_4 [24-55]. Its hydrogenation properties are thought to be strongly affected by its nanometer scale structures by means of thermodynamic and kinetic aspects. Zalusky et al. [24] and Orimo et al. [25] have shown that absorption/desorption properties of nanocrystalline Mg_2Ni alloys mechanically alloyed at low temperatures can be enhanced by grain size reduction. Furthermore, it has been demonstrated that catalysts and ball milling [25-30] utilization provide a faster kinetics of hydrogenation/dehydrogenation. It thus represents one of the most common approaches for improving the magnesium hydride behavior in hydrogen absorption. The synthesis process "reactive mechanical alloying" (RMA) combines these two very important aspects. Then, kinetics improvements and a decrease of the decomposition temperature can be obtained with both chemical alloying and material processing (melt spinning, mechanical alloying) [31-43]. Zhang et al. [44-47] produced Mg_2Ni-type alloys as $Mg_2Ni_{(1-x)}Co_x$, $Mg_2Ni_{(1-x)}Cu_x$ and $Mg_2Ni_{(1-x)}Mn_x$ (x = 0, 0.1, 0.2, 0.3, 0.4) by melt spinning technique, obtaining an almost complete desorption of hydrogen in 20 minutes with a quantity of hydrogen desorbed ranging from 0.5 and 2.3 weight % as a function of spinning rate and Co, Cu and Mn concentrations. Iturbe-Garcıa et al. [48] studied the behavior along the temperature range from 25 to 350 °C of Mg_2Ni-hydrides obtained by mechanical alloying. The maximum hydrogen amount desorbed was 3.95 weight % in about 15 min. Oelerich et al. [48] claim to have obtained hydrogen desorption in about 5 minutes at 227 °C and in 1 minute at 300 °C substituting partially Ni with Cu and milling for 100 h. E. Grigorova et al. [49] obtained the dehydrogenation kinetic curve at 300 °C and 1.5 atm of the following composite 85 wt.% Mg_2Ni–10 wt.%V–5 wt.% Ti produced by mechanical alloying. They reached an almost complete desorption of hydrogen in 10 minutes with a quantity of hydrogen desorbed of about 2 weight %. Song et al [50] reported the results on dehydrogenation behaviors in a temperature range of 250–350 °C obtained by porous $Mg_{67}Ni_{(33-x)}Y_x$ (x = ¼ 0, 1, 3, 6) ribbons which are prepared by a melt spinning method. They obtained an

almost complete desorption of hydrogen in 2-10 minutes with a quantity of hydrogen desorbed ranging from 1 and 3.6 weight % as a function of Y concentration and temperature. Mg-Ni alloys having RE as catalyst have been, also, synthetized in order to lower the absorption temperature [52-55]. Spassov *et al*. [51-53] also confirmed that melt spinning could significantly improve the hydrogen absorption/desorption performance of Mg-based alloy, to obtain a maximum hydrogen capacity of 4.0 wt % H for the as-spun $Mg_{75}Ni_{20}Mm_5$ (Mm: "misch metal" with Ce and La) alloy. Li [54] investigated the structure and hydrogen storage properties of $Mg_{1.7}NiM_{0.3}$ (M = Mg, La, Nd and Ce) composites. Comparing to Mg_2Ni, the substitution of Mg with RE metals, even if decreases hydrogen capacities of the alloys, enhances significantly the hydrogen absorption and desorption rates.

Tanaka [55] shows that the nanocrystallization of melt-spun amorphous alloys of the Mg–Ni–RE systems is one of the prospective approaches to obtain a good hydriding–dehydriding kinetics for hydrogen energy systems. In this contest, the aim of this study are both to synthesize, by a melting process and ball milling, a Mg-Ni-RE alloy by using a commercial alloy, named "Firesteel" instead of "mish metal", and to make a comparison with results found in literature up to 350 °C. Moreover, plenty of thermodynamic data about the hydrogen desorption/absorption processes of hydrides under equilibrium are available in literature, but very few are those referred to real conditions (far from equilibrium and controlled by kinetics) in which hydrides usually absorb and desorb hydrogen, extremely important for practical application. The intention is to investigate the real performances of hydride by taking into account the dynamic conditions studied in a mass flow measurement system, instead than in static conditions. Then, data collected in this work are more related to kinetic rather than thermodynamic properties of the material.

2. Experimental

2.1.Instruments

The alloy has been produced by melting technique in an induction furnace (Manfredi Neutor Digital) in an argon protective atmosphere, using a silica vitreous crucible. The furnace is equipped with a centrifugal casting system. Specimens have been cast in a graphite mold and the mold temperature was kept at 25°C. A hydraulic press "Beckman", with a press force of 12 tons per cm^2 has been used to crush the alloy and a ball mill equipped with steel balls with a diameter of 20 mm (planetary micro mill PULVERISETTE 7, Fritsch) has been utilized to grind it, under argon.

The alloys compositions have been analyzed by a Scanning Electron Microscope (Hitacy S 2500) equipped with EDS probe (Kevex mod 3600-0400, software Noran System Six)), while X-ray

diffraction (Philips PW 1830 GENERATOR Cu-Kα radiation λ=0.15418 nm) has been performed on synthesized and cycled samples, for studying the phase composition.

Simultaneous thermogravimetry and differential scanning calorimetry (TGA-DSC) experiments were carried out on about 10-12 mg of powder after hydrogenation, using a Stanton-Redcroft 625 apparatus operating through a Rheometric Scientific system interface controlled by the software RSI Orchestrator. A constant rate of 10°C min^{-1} under a flowing argon atmosphere of 50 ml min^{-1} has been used, by means of two identical open cylindrical alumina crucibles (one for the sample and one for the reference) until 600°C. A very pure indium reference sample was used for calibration of temperature, that has been estimated with a final uncertainties of ±0.1°C .

BET (Fisons instruments) analyses have been, also, performed at nitrogen liquid temperature and using N_2 gas to evaluate the specific surface of powders.

The Pressure Composition Temperature (PCT) curves of $Mg_{68}Ni_{26}M_5X$ alloy have been obtained employing a mass flow measurement apparatus "MFM" (made by IONVAC process *srl*), displayed in figure 1, where is shown as it works: the hydrogen flows through 6-mm-diameter steel pipes starting from a pressurized tank (200 atm) located outside the building. A special pressure reducer, located near the tank, allows keeping the line pressure at 18–20 atm (limit pressure of the system), while a further pressure regulator PCV-2 ensures a lower pressure maintaining. After passing the pressure-reducing valve V2, hydrogen flows through the valve V3 and meets the first 'T' junction. From this point on, it can proceed in the flowmeter (MFC; Bronkhorst; range: 0-100 Nml/min) direction during charging, when the valves V6, V7 and V4 are closed and V5 is open. Alternatively, it can flow back through the valve V6 during the discharge, when the valves V3, V4 and V5 are closed, and allowing the passage through the flowmeter and the valve V7. The filters F1 and F2 prevent powdered hydrides damage the flowmeter. The system can measure the flow, pressure and temperature in the storage system of hydrides. Pressure and temperature can be controlled. The National Instruments data acquisition system (Field Point) that collects the signals and sends them to a computer, where a LabVIEW program displays and records the data. The flow rate in the discharge step could also be different from that of the charging step, until the atmospheric pressure was reached; the vacuum pump was then activated in order to reset the starting operating conditions for the next cycle. In any case it was verified that the hydrogen quantity passing through the flowmeter by vacuum pump was very negligible with respect to the overall capacity of the Mg-Ni-M alloy. After each discharge, a steady flow of hydrogen was sent into the test circuit containing the sample to carry out the charge, until the highest pressure value preset (about 11 atm) was achieved.

2.2. Synthesis of the alloy

The $Mg_{84}Ni_{14}M_{1.5}X_{0.5}$ master alloy, has been produced employing pure elements (Ni powder 99.995% Sigma-Aldrich, Mg chips 99.980% Sigma-Aldrich) and "Firesteel" (commercial alloy containing 38.0% of La, 43.4% of Ce, 11.7% of Fe and minor amounts of Si, Al and Mg) as starting materials. Since magnesium is pyrophoric, it was necessary to work in an oxygen free atmosphere. Another problem arises from the boiling point of magnesium (1090°C), which is significantly lower than nickel melting temperature (1455°C). Thus, magnesium lost during the melting process can be expected. Taking into account these chemical-physical properties it has been decided to melt first a master alloy, under argon atmosphere, having composition as close as possible to the desired composition, but considering the actual magnesium losses, a significant excess of this element has been introduced into the furnace ceramic crucible. Precisely, 10.5 g of Mg, 6.5 g of Ni and 3.0 g of "Firesteel" have been melted together. The total initial weight of the elements was 20 g, at the end of this first melting step the obtained alloy weight was 7.5 g with a mass loss of about 63%. However, during the melting process the magnesium lost has been less than that foreseen, while a loss of Ni and M has been recorded proportionally to their initial stoichiometry, likely owing to the formation of an eutectic between Ni and Mg [55]. To reach the desired composition the master alloy has been, then, re-melted in a second step, with the addition of 1.2 g of nickel and 1.9 g of "firesteel". The master and re-melted alloy compositions have been, therefore, analyzed by Scanning Electron Microscope equipped with EDS probe. Table 1 reports the chemical composition of two alloys, showing that more than one step has been needed to produce a particular alloy composition. In this case two steps are enough. As shown by EDS analysis on master and final alloys, the concentration of Mg decreases while those of Ni and M increase, approaching the desired composition. Eventually it has been obtained an alloy quite similar to the target, with a composition $Mg_{68}Ni_{26}M_5X$ where X represents Si and Fe, whose presence is due to the "Firesteel" alloy. First the final alloy has been crushed 6 times under argon atmosphere (in a dry box), by means of the hydraulic press and then grinded, under argon, using the ball mill. The grinding process has been, also, repeated 6 times with 10 minutes of grinding step and 5 minutes break between each grinding step and the next one. The rotation speed was 500 rpm.

3. Results and discussion

3.1. SEM analyses

As shown in figure 2 the particles of fresh milled powder, having a completely smooth surface, are not homogeneous in sizes, furthermore the SEM observation highlights that most of the particles belongs to the dimensional range 5-70 μm, with few isolated much larger particles (up to 300 microns). After activation process followed by some cycles of hydrogen reaction inside the MFM

apparatus, the powder samples were observed by SEM. The micrographs are reported in figure 3. By comparing these micrographs with those of figure 2 a decreasing of the particle size and a metallic aspect reduction with sponginess increase can be immediately observed. That last observation is particularly evident in figure 3 at higher magnifications.

3.2. BET analysis

The results of BET analysis, performed on both the fresh powder (just synthesized) and the sample obtained after activation and cycling, confirmed, as expected, the findings of SEM analyses on the same samples. In fact, it is worth noting that the specific surface area of the freshly prepared sample, equal to 1.5 $m^2 g^{-1}$, increased to about 10 $m^2 g^{-1}$ after cycling.

3.3. Absorption-Desorption

The absorption-desorption capability of the Mg-Ni-M alloy has been verified by charge and discharge cycles performed for both allowing its activation and studying the process kinetics. Therefore, fresh milled powder has been introduced inside the MFM apparatus, by which early charging and discharging cycles were performed at 300°C observing a progressive activation. Successively, reversible absorption-desorption capability of the alloy Mg-Ni-M has been verified, between 300°C and 350 ^{o}C respectively.

The 11 cycles of charging and discharging were performed in the following experimental conditions:

- Temperature was maintained constant, inside the reactor, during each hydrogenation and dehydrogenation cycle at different values in the range 300 ÷ 350°C. in particular, in the early cycles, the desorption temperature was maintained equal to that of absorption, observing a progressive activation. In the last cycles, instead, a desorption temperature different from that of absorption was used;
- Maximum hydrogen pressure, inside reactor was equal to 11atm;
- Flow rate was equal to about 10 $NmLmin^{-1}$ for absorption;
- Flow rate was equal to about 7.5 $NmLmin^{-1}$ for desorption;
- Powder sample mass was of 2.5 g.

Therefore, introducing 2.5 g of powder sample into MFM system, the graphs in figures 4 and 5 have been obtained; they show, respectively, the more representative curves of hydrogen charging and discharging in the above reported experimental dynamic conditions. By observing figure 4 a) and b) it is evident that the thermal treatment above 300°C causes the activation of the compound. It is also shown that at 300°C, the alloy activation is slow, but it increases after every cycle. Indeed, in the first cycle the virtual absence of absorption is demonstrated by the lack of plateau, or however, the inflection of the curve, while in the 9^{th} cycle (performed at the same temperature,

196 pressure and flow rate conditions), an increased absorption is evident, as it can be qualitatively
197 detected by both the test duration and the three inflections in the absorption curve. In all the cycles
198 the hydrogen content desorbed is always a bit lower, even if quite similar, to that absorbed.
199 When the 11^{th} cycle has been reached, the conditions for an excellent absorption are obtained.
200 Furthermore, at that temperature it is possible to observe three different absorption steps,
201 respectively at about 3, 4 and 7 atm pressure. 0.15% of involved hydrogen, takes place at 3 atm and
202 could be attributed to superficial absorption, while the second and third stages, involving 0.4 and
203 2.2 % of hydrogen (at pressures of 4 and 7 atm, respectively) are related to formation of different
204 hydride phases like MgH_2 and Mg_2NiH_4 as reported in previous studies [19,20,54]. By considering
205 11^{th} curve of figure 5 it is important to highlight that the increase of pressure is related to hydrogen
206 desorption kinetics higher than hydrogen flow fixed by the flowmeter (no static but dynamic
207 conditions, therefore no thermodynamics but kinetics conditions).
208 It is possible to affirm that taking into account the hydrogen specific energy of about 140 MJ/kg
209 and by using a flow rate of 7.5 $NmLmin^{-1}$, the alloy is able to deliver 625 $J \cdot s^{-1} \cdot kg^{-1}$ and, therefore,
210 by a fuel cell having an efficiency η equal to 0.5, to produce a power of around 310 W per kg of
211 hydride for about 2 hours.
212 *3.4. Thermal and kinetics analyses*
213 TGA-DSC curves, show in figure 5 that hydrogen desorption occurs in the temperature range
214 between 310 and 375°C, with a mass loss of about 3.8 %, but by hydrogen desorption up to 350 °C
215 is accompanied by a mass loss of 2.7 %. It means that some irreversibly accumulated hydrogen,
216 along the cycling process between 300 °C and 350 °C, can be desorbed only if the temperature
217 overcomes 350 °C. A strong dehydrogenation requires working temperature close to 375°C, giving
218 a maximum of desorbed hydrogen equal to 3.8%, while just 2.7 % of hydrogen can be desorbed in a
219 reversible way up to 350 °C, which is the temperature corresponding to the highest process rate
220 (flex of the de-hydrogenation TGA curve: point A of figure 5).
221 The desorption kinetics is reported in figure 6, where it is shown that the hydride reaches 3.8% of
222 hydrogen desorption in about six minutes. Indeed, as demonstrated in literature [41-55], it can be
223 expected that the presence of heteroatoms in Mg-Ni alloys can have positive effects on the
224 desorption kinetics.
225 In order to find the activation energy for hydrogenation/dehydrogenation processes a kinetic
226 analysis of the thermal dehydrogenation of the Mg-Ni alloy tested was performed by processing
227 dynamic TG data at different heating rates β (at least four experiments), according to the well-
228 known Kissinger and Kissinger-Akahira-Sunose (KAS) methods, whose details are given elsewhere
229 [56,57]. Heterogeneous processes involving solid and gas species in reacting or inert atmosphere

require a more exhaustive kinetic analysis than those used for homogeneous processes. In particular, the energy barrier (activation energy) that reagents must overcome for the former reactions cannot (and usually must not) be constant during its occurrence. The former method gives a single value of activation energy for the whole process, while the latter provides a value of activation energy for each value of the extent of reaction α, defined as:

$$\alpha = (m_i - m_t)/(m_i - m_f) \quad (1)$$

where m_i, m_f and m_t are the initial, final and the mass (in mg) corresponding to a defined temperature T, respectively.

Thus, once a single activation energy (E_a) value is obtained for the whole dehydrogenation process by the Kissinger method (151±8 kJ mol^{-1}) from the slope of the regression line in figure 7a, a typical α-dependency of activation energy is provided using the KAS isoconversional method in figure 7b. A moderate increasing trend is observed with increasing the extent of reaction alpha in a wide range of alpha (from 0.1 to 0.8), and a mean value can be considered because its negligible variation is comparable with the associated estimated uncertainties (around 8-10%). This mean value, 158 ±11 kJ mol^{-1}, is in excellent agreement with the single value previously estimated.

3.5 X-ray analyses

The X-ray (Philips CuK_α radiation) diffractogram of crude, hydrogenated and dehydrogenated hydride are displayed in figures 8a), 8b) and 8c) respectively.

The pattern of the crude powder synthesized shows the peaks related to polycrystalline Mg_2Ni compound and Mg, while after hydrogenation two phases are present in agreement with what has been previously reported in literature [18, 22]: Mg_2NiH_4 and MgH_2.

After the subsequent dehydrogenation the presence of Mg_2NiH_4, as well as those of MgH_2 and Mg_2Ni, is still evident. Furthermore, dehydrogenation occurring during the cycling is not complete, owing to temperature adopted (350°C), indeed from TGA/DSC analysis the complete dehydrogenation temperatures are found to be higher than 350°C and then, up to 350 °C, hydrogen content still remains [42,43]. Moreover, because of during the measures the powder has been exposed to air and humidity, the presence of MgO and $MgCO_3$ has been revealed resulting from the reaction between highly reactive Mg, after dehydrogenation, and oxygen and carbon dioxide present in air [58,59].

4. Conclusions

The alloy with general formula $Mg_{68}Ni_{26}M_5X$, using a commercial alloy named “Firesteel”, has been prepared by a two-step process in an induction furnace equipped with a centrifugal casting system and used in hydrogenation-dehydrogenation experiments. A first melting step is needed to produce a master alloy more easily usable than pure metals, while a second melting step is

necessary to both adjust alloy composition and prevent further Mg losses. The alloy has been, then, grounded with a ball mill in order to increase both the surface/volume ratio and the surface defects. Tests performed on the sample $Mg_{68}Ni_{26}M_5X$ showed that:

- The hydride activation is obtained at 300°C. At this temperature, even if the activation is slow, it increases after every cycle. The pressure value is about 11 atm.
- After activation, the hydrogen absorption occurs at 300°C in three stages at three different pressures: the first stage of absorption involving 0.15% of hydrogen takes place at 3 atm and could be attributed to surface absorption. The second and third stages, involving 0.4 and 2.2% of hydrogen at 4 and 7 atm, respectively, are related to formation of different hydride phases: MgH_2 and Mg_2NiH_4.
- Results of TGA/DSC measurements highlight that strong dehydrogenation of the hydrogen accumulated in an irreversible way, requires working at temperature close to 375°C, giving 3.8% of desorbed hydrogen, while 2.7 % of hydrogen can be desorbed up to 350 °C in a reversible way.
- The temperature desorption presenting a faster kinetic is about 350 °C.
- X-rays performed on the raw and cycled material (in the range 300-350°C) showed that Mg_2Ni and Mg contained in the raw material is transformed into Mg_2NiH_4 and MgH_2 after hydrogenation. Both phases revert reversibly at 350°C, only partially in Mg_2Ni and Mg.
- For practical application it has been verified that the alloy is able to deliver, at 350 °C, during the hydrogen discharge a flow rate of 7.5 $NmLmin^{-1}$, assuring by a fuel cell having an efficiency η equal to 0.5, a power of around 310 W per kg of hydride, for about 2 hours.
- Good results have been obtained, comparing them with those found in literature and considering a maximum temperature of 350 °C as reference.

References

[1] Chandra D. Solid-state hydrogen storage, materials and chemistry, edited by Gavin Walker, Woodhead Publishing Limited, Cambridge England, 2008.

[2] Varin RA, Czujko T, and Wronski ZS, Nanomaterials for Solid State Hydrogen Storage Springer Science Business Media, LLC, 233 Spring Street, New York, NY 10013, USA 2009

[3] Huot J. Handbook of Hydrogen Storage: New Materials for Future Energy Storage Edited by Michael Hirscher New Materials for Future Energy Storage WILEY-VCH Verlag GmbH & Co. KGaA, Weinheim, 2010.

[4] Broom DP, Hydrogen storage materials, the characterization of their storage properties, Springer-Verlag London Limited, DOI 10.1007/978-0-85729-221-6, 2011.

[5] Westerwaal R.J, Haije WG. Evaluation solid-state hydrogen storage systems. Hydrogen and Clean Fossil Fuels, 2–75, 2008.

[6] K.H.J. Buschowin: K.A. Gschneidner Jr., L. Eyring (Eds.), Handbook on the Physics and Chemistry of Rare Earths, Vol. 6, Elsevier, Amsterdam (1984) Chapter 47

[7] T. Sakai in: K.A. Gschneidner Jr., L. Eyring (Eds.), Handbook on the Physics and Chemistry of Rare Earths, Vol. 21, Elsevier, Amsterdam (1995) Chapter 142

[8] Al-Hallaj S, Kiszynski K. Hybrid. Hydrogen Systems. Stationary and Transportation Applications. Springer-Verlag London Limited 2011.

[9] Schlapbach L, Züttel A. Hydrogen-storage materials for mobile applications. Nature 2001;414:353-358,

[10] Bocci E, Zuccari F, Dell'Era A. Renewable and hydrogen energy integrated house. Int J Hydrogen Energ. 2011;36:7963-7968

[11] Orecchini F, Santiangeli A, Dell'Era A. A Technological Solution For Everywhere Energy Supply. J Fuel Cell Sci Tech. 2006;3:75-82

[12] De Rosa IM, Dell'Era A, M. Pasquali, Santulli C, Sarasini F. Acoustic emission monitoring of activation behavior of LaNi5 hydrogen storage alloy. Sci Technol Adv Mat. 2011, 12,

[13] D'orazio A, Dell'Era A, Artuso P, Pasquali M. Hydride tank storage system dimensioning on the base of their dynamic behavior. Int J Hydrogen Energ. 2011; 36:7902-7908

[14] Selvam P, Viswanathan B, Swamy CS and Srinivasan V. Magnesium and magnesium alloy hydrides. Int J Hydrogen Energ, 1986;11:169 –192.

[15] Saita I, Toshima T, Tanda S, Akiyama T. Hydrogen storage property of MgH_2 synthesized by hydriding chemical vapor deposition. J Alloy Compd. 2007; 446:44780–83

[16] Fujii H, Orimo S, Ikeda K.Cooperative hydriding properties in a nanostructured Mg_2Ni–H system J. Alloys Compd, 1997; 253: 80-83.

[17] Orimo S, Fujii H. Materials science of Mg–Ni-based new hydrides. Appl Phys A 2001;72:167–186.

[18] Urretavizcaya G., García G., Serafini D. and Meyer G.. Mg-Ni alloys for hydrogen storage obtained by ball milling. Latin Am Appl Res. 2002;32:289-294

[19] Ikeda Y, Ohmori T. Study on chemical synthetic method to prepare Mg_2Ni hydrogen absorbing alloy. Int J Hydrogen Energ, 2009; 34:5439-5443.

[20] Jianxin Zou, Haiquan Sun, Xiaoqin Zeng, Gang Ji andWenjiang Ding, Preparation and Hydrogen Storage Properties of Mg-Rich Mg-Ni Ultrafine Particles, J Nanomater 2012;8 pages, doi:10.1155/2012/592147

[21] Hagstrom MT, Lund PD and Vanhanen JP. Metal hydride hydrogen storage for near-ambient temperature and atmospheric pressure applications, a PDSC study, Int J. Hydrogen Energ, 1995;20, 2:897-909.

[22] Polanski M, Nielsen TK, Kunce L, Norek M, Płocinski T, Jaroszewicz LR, Gundlach C, Jensen TR, Bystrzycki J. Mg_2NiH_4 synthesis and decomposition reactions, Int J Hydrogen Energ 2013;38,10:4003-4010.

[23] Niaz NA, Ahmad I, Khan WS and Hussain ST, Synthesis of Nanostructured Mg-Ni Alloy and Its Hydrogen Storage Properties, J Mater SciTechnol, 2012;28,5:401-406.

[24] Orimo S, Fujii H, Ikeda K. Notable hydriding properties of a nanostructured compositematerial of the Mg_2Ni-H system synthesized by reactive mechanical grinding. Acta mater. 1997;45:331 – 341.

[25] Zalusky L, Zaluska A, Tessier P, Ström-Olsen JO, Schulz R. Hydrogen absorption in nanocrystalline Mg_2Ni formed by mechanical alloying. J Alloys Compd. 1995; 217:245 – 249

[26] Sharbati M and Kashani-Bozorg SF. Evolution of Nanocrystalline Structures Using High Energy Ball Milling of Quaternary $Mg_{1.75}Nb_{0.125}C_{0.125}Ni$ and Binary Mg_2Ni, Proceedings of the International Congress on Advances in Applied Physics and Materials Science, Antalya 2011, Acta Phys Pol A 2012;121:211-213

[27] Martínez–Franco E, Klassen T, Jaramillo–Vigueras D, Bormann R, Hydrogen Sorption Properties of the Intermetallic Mg_2Ni Obtained by Using a Simoloyer Ball Milling, Ing Invest Tecnol, 2010;11,3:325-332

[28] Barkhordarian G, Klassen T. and Bormann R. Kinetic investigation of the effect of milling time on the hydrogen sorption reaction of magnesium catalyzed with different Nb_2O_5 contents. J Alloys Compd, 2006;407:249–255.

[29] Varin RA, Czujko T. Overview of processing of nanocrystalline hydrogen storage intermetallics by mechanical alloying/milling. Mater. Manuf. Proc. 2002;17: 129 – 156.

[30] Wronski Z, Varin RA, Chiu C, Czujko T, Calka A. Mechanochemical synthesis of nanostructured chemical hydrides in hydrogen alloying mills. J. Alloys Compd 2007; 434: 743 – 746.

[31] Oelerich W, Klassen T, Bormann R. Comparison of the catalytic effects of V, V_2O_5, VN, and VC on the hydrogen sorption of nanocrystalline Mg. J. Alloys Compd. 2001;322:L5 – L9.

[32] Li F, Jiang L, Du J, Wang S, Liu X, Zhang F. Investigations on synthesis and hydrogenation properties of Mg-20wt%Ni-1wt%TiO_2 composite prepared by reactive mechanical alloying. J. Alloys Compd. 2008;452:421–424.

[33] Wang L, Yang RT. New sorbents for hydrogen storage by hydrogen spillover–a review. Energy Environ Sci 2008;1:268–279

[34] Cheng H, Chen L, Cooper AC, Sha X, Pez GP. Hydrogen spillover in the context of hydrogen storage using solid-state materials. Energy Environ Sci 2008;1:338–354

[35] Varin RA, Lia S, Calkab A, Wexlerb D. Formation and environmental stability of nanocrystalline and amorphous hydrides in the 2Mg–Fe mixture processed by controlled reactive mechanical alloying (CRMA). J Alloys Compd, 2004; 373(1–2): 270–286.

[36] Gennari FC, Castro FJ, Urretavizcaya G. Hydrogen desorption behavior from magnesium hydrides synthesized by reactive mechanical alloying. J Alloys Compd. 2001; 321:46 – 53 .

[37] Varin RA, Li S, Chiu C, Guo L, Morozova O, Khomenko T, Wronski Z. Nanocrystalline and non-crystalline hydrides synthesized by controlled reactive mechanical alloying/milling of Mg and Mg-X (X = Fe, Co, Mn, B) systems. J. Alloys Compd. 2005;404-406: 494-498.

[38] Gennari FC, Castro FJ, Andrade Gamboa JJ. Synthesis of Mg_2FeH_6 by reactive mechanical alloying: formation and decomposition properties. J. Alloys Compd. 2002;339:261- 267 .

[39] Bobet JL, Chevalier B, Song MY, and Darriet B. Improvements of hydrogen storage properties of Mg-based mixtures elaborated by reactive mechanical milling. J. Alloys Compd. 2003; 356: 570-574.

[40] Iturbe-Garcıa JL, Lopez-Munoza BE, Basurto R, and Millan S, Hydrogen desorption process in Mg_2Ni hydrides, Rev Mex Fis 2006;52, 4:365-367.

[41] Cermak J, Kral L, Beneficial effect of carbon on hydrogen desorption kinetics from Mg–Ni–In alloy, J. Alloys Compd 2013;546:129–137.

[42] Sabitu ST and Goudy AJ, Dehydrogenation kinetics and modeling studies of MgH_2 enhanced by transition metal oxide catalysts using constant pressure thermodynamic driving forces, Metals 2012;2:219-228.

[43] Beattie SD, Setthanan U, McGrady GS, Thermal desorption of hydrogen from magnesium hydride (MgH_2): An in situ microscopy study by environmental SEM and TEM, Int J. Hydrogen Energ, 2011;36,10:6014–6021.

[44] Zhang B, Lu Y, Yuan J, WuY Effects of Microstructure on the hydrogen storage properties of the melt-spun Mg-$_5$Ni-$_3$La (at.%) alloys, J. Alloys Compd 2017;702:126-131

[45] Zhang YH, Zhao DL, Li BW, Ren HP, Guo SH, Wang XL Hydriding and dehydriding kinetics of melt spun nanocrystalline $Mg_{20}Ni_{10-x}Cu_x$ (x = 0-4) alloys, Nat Sci, 2010;2,1:18-25

[46] Zhang YH, Zhai T, Li B, Ren H, Bu W, Zhao D. Highly Improved Gaseous Hydrogen Storage Characteristics of the Nanocrystalline and Amorphous Nd-Cu-added Mg_2Ni-type Alloys by Melt SpinningmJ. Mater. Sci. Technol., 2014;30,10:1020-1026

[47] Zhang YH, Li BW, Ren HP, Li X, Qi Y and Zhao DL. Enhanced Hydrogen Storage Kinetics of Nanocrystalline and Amorphous Mg_2Ni-type Alloy by Melt Spinning, Materials 2011, *4*, 274-287; RSC Adv., 2015;5:54258–54265

[48] Oelerich W, Klassen T, Eigen N, Bormann R, Nanocrystalline Metal Hydrides for Hydrogen Storage Functional Materials, ed. by K. Grassie, E. Teuckhoff, G. Wegner, J. Haußelt, H. Hanselka, Wiley-VCH, Weinheim 2000, Euromat 13, 141-145.

[49] Grigorova E, Khristov M, Khrussanova M, Peshev P. Addition of 3d-metals with formation of nanocomposites as a way to improve the hydrogenation characteristics of Mg_2Ni. J Alloys Compd 2006;414:298-301

[50] Song W, Li J, Zhang T, Hou X and Kou H. Dehydrogenation behavior and microstructure evolution of hydrogenated magnesium–nickel–yttrium melt-spun ribbons. RSC Adv, 2015;5:54258–54265

[51] Spassov T, Koster U Hydrogenation of amorphous and nanocrystalline Mg-based alloys. J Alloys Compd, 1999;287:243–250

[52] Spassov T, Rangelova V, Neykov N. Nanocrystallization and hydrogen storage in rapidly solidified Mg–Ni–RE alloys J. Alloys Compd, 2002;334:219–223

[53] Spassov T, Lyubenova L, Kösterc U, Barób MD. Mg–Ni–RE nanocrystalline alloys for hydrogen storage. Mat Sci Eng A, 2004;375–377:794–799

[54] Li Y, Li P, Zhai F, Zhang W, Qu X. Hydrogen storage properties of $Mg_{1.7}M_{0.3}Ni$(M=Mg, La, Ce, Nd）hydrogen storage alloys. Adv Mat Res 512-515:1503-1508

[55] Tanaka K, Kanda Y, Furuhashi M, Saito K, Kuroda K, Saka H Improvement of hydrogen storage properties of melt-spun Mg–Ni–RE alloys by nanocrystallization J. Alloys Compd 1999;293–295:521–525

[56] Akahira T, Sunose T, Method of determining activation deterioration constant of electrical insulating materials, Res. Report Chiba Inst. Technol. Sci Technol, 1971;16:22–31.

[57] Duce C, Vecchio Ciprioti S, Ghezzi L, Ierardi V, Tinè MR, Thermal behavior study of pristine and modified alloysitenanotubes.A modern kinetic study. J Therm Anal Calorim 2015;121:1011-1019.

[58] Fricker KJ and Alissa Park AH, Effect of H_2O on $Mg(OH)_2$ Carbonation Pathways for Combined CO_2 Capture and Storage, Chem Eng Sci 2013;100:332-341

[59] Ogawa S, Niwa H, Nakanishi K, Ohta T, and Yagi S. Influence of CO_2 and H_2O on Air Oxidation of Mg Nanoparticles Studied by NEXAFS, J Surf Anal, 2011;17, 3:319-323

Figure list

Table list

Table

Table 1 Atomic composition of master and final alloy from EDS analyses

	Master alloy composition	Re-melted alloy composition
Element	Atom %	Atom %
Mg	84.2	67.9
Si	0.1	0.3
Fe	0.3	0.8
Ni	14.1	25.8
La	0.5	2.2
Ce	0.8	3.0
Total	100.0	100.0

Figure 1

Click here to download high resolution image

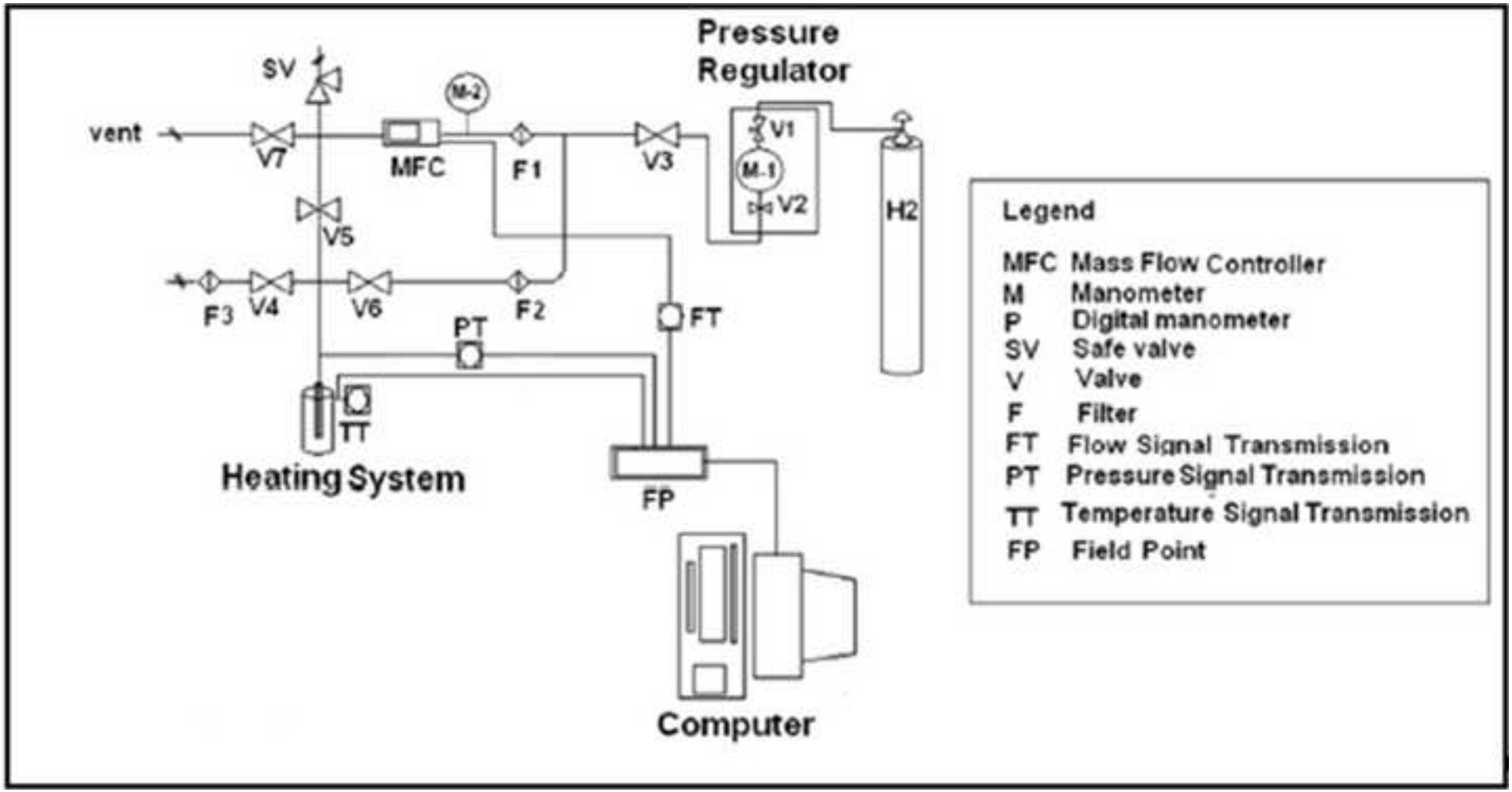

Figure 2

Click here to download high resolution image

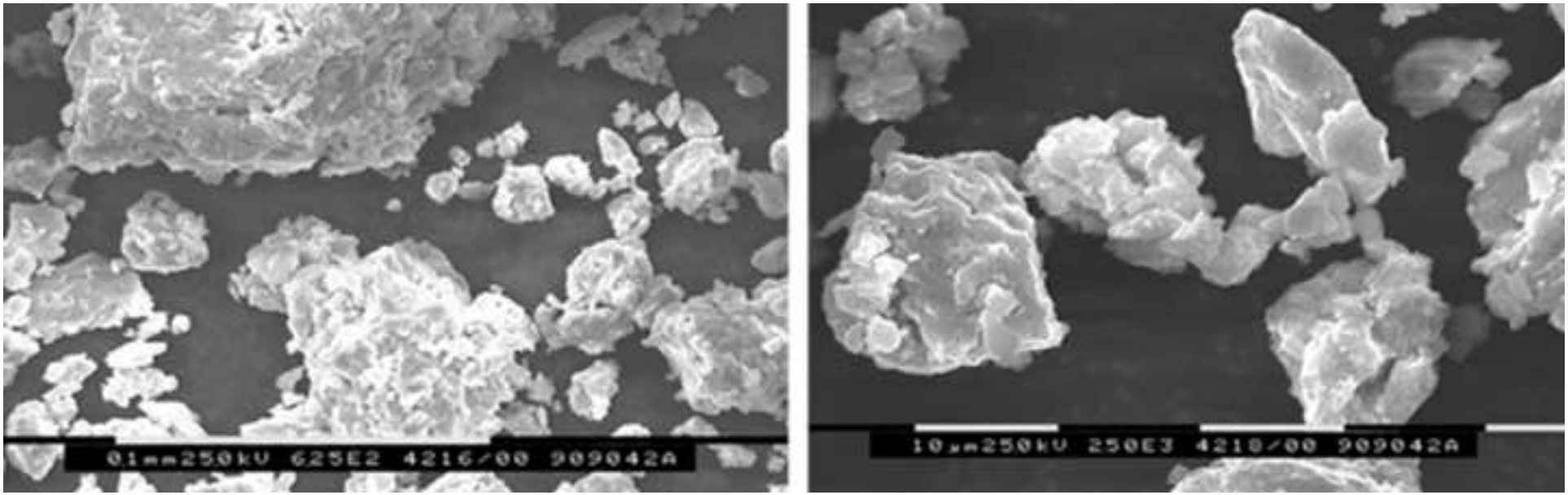

Figure 3

Click here to download high resolution image

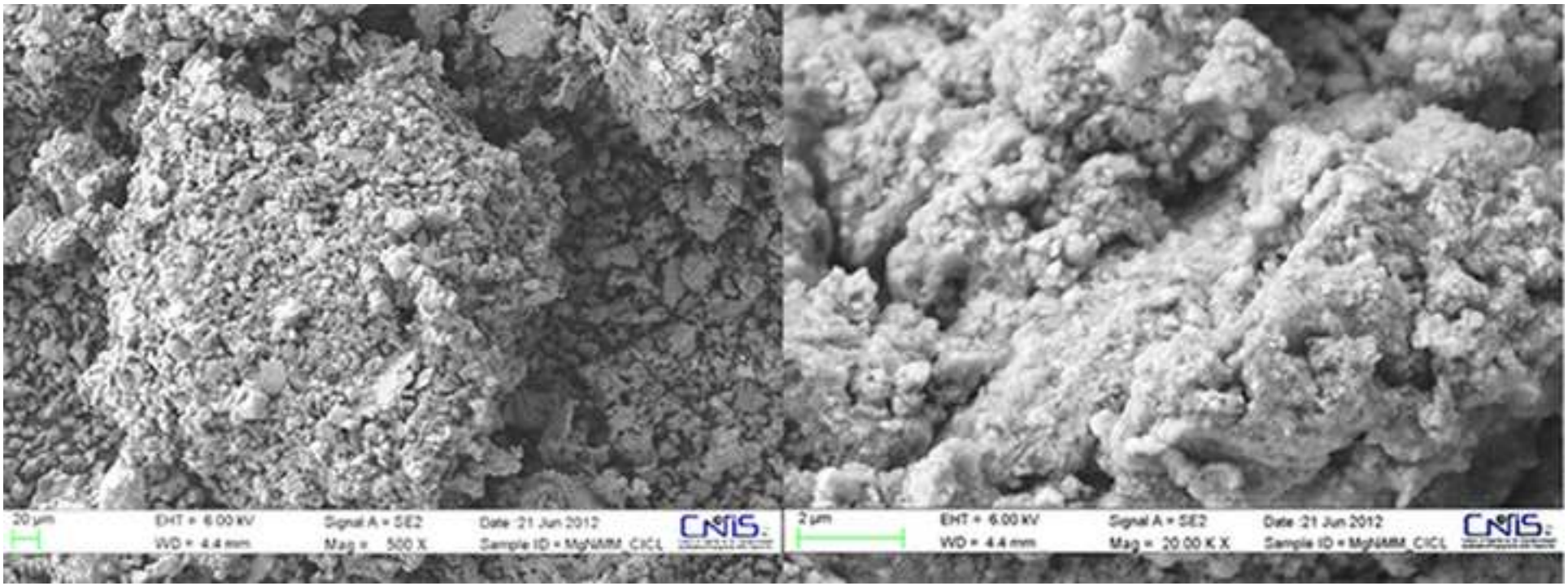

Figure 4

Click here to download high resolution image

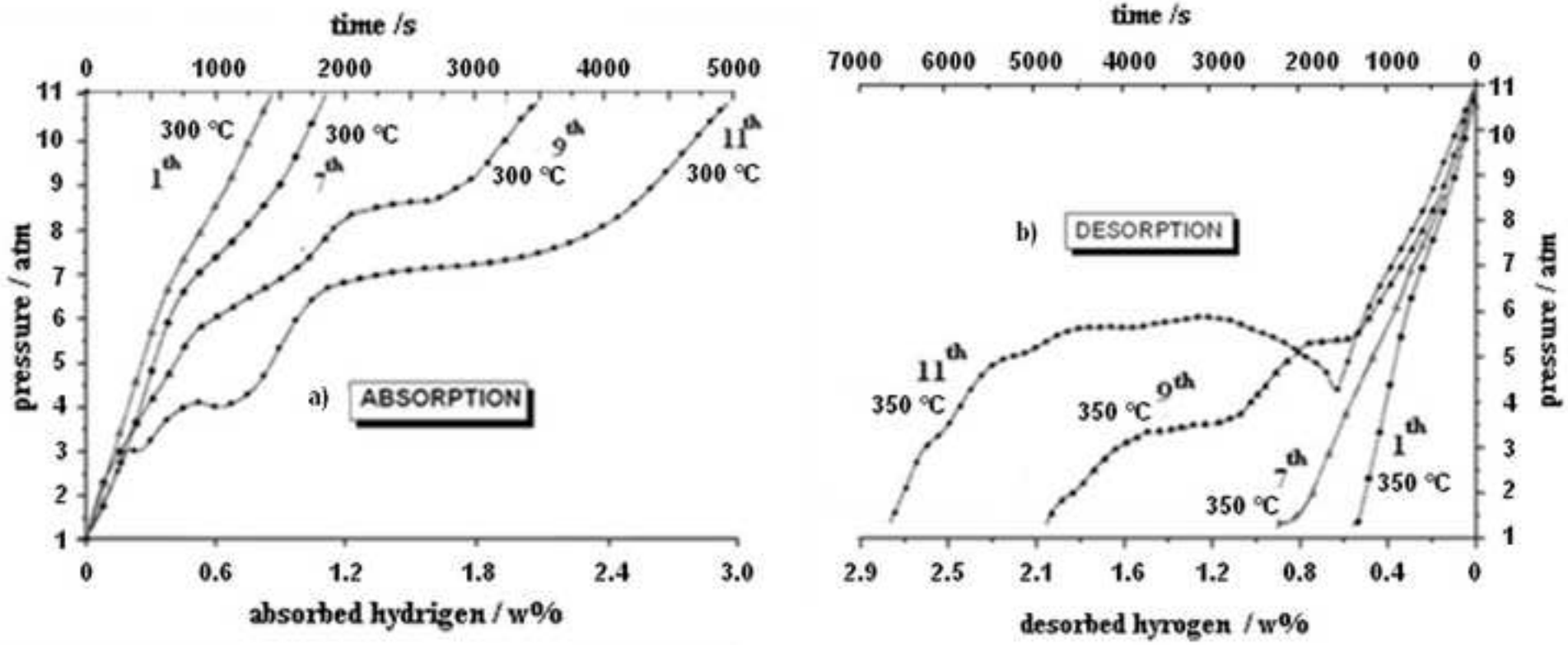

Figure 5

Click here to download high resolution image

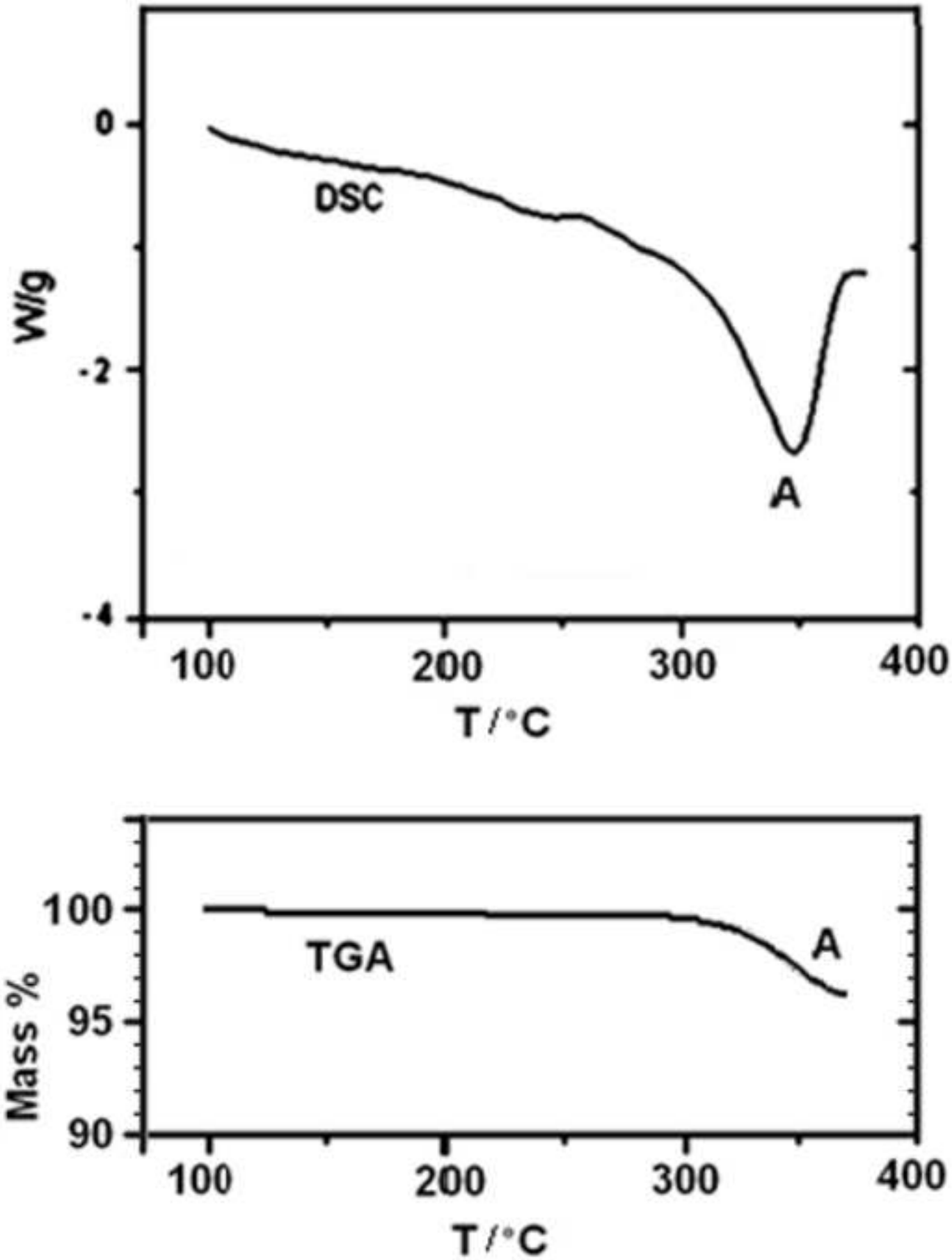

Figure 6

Click here to download high resolution image

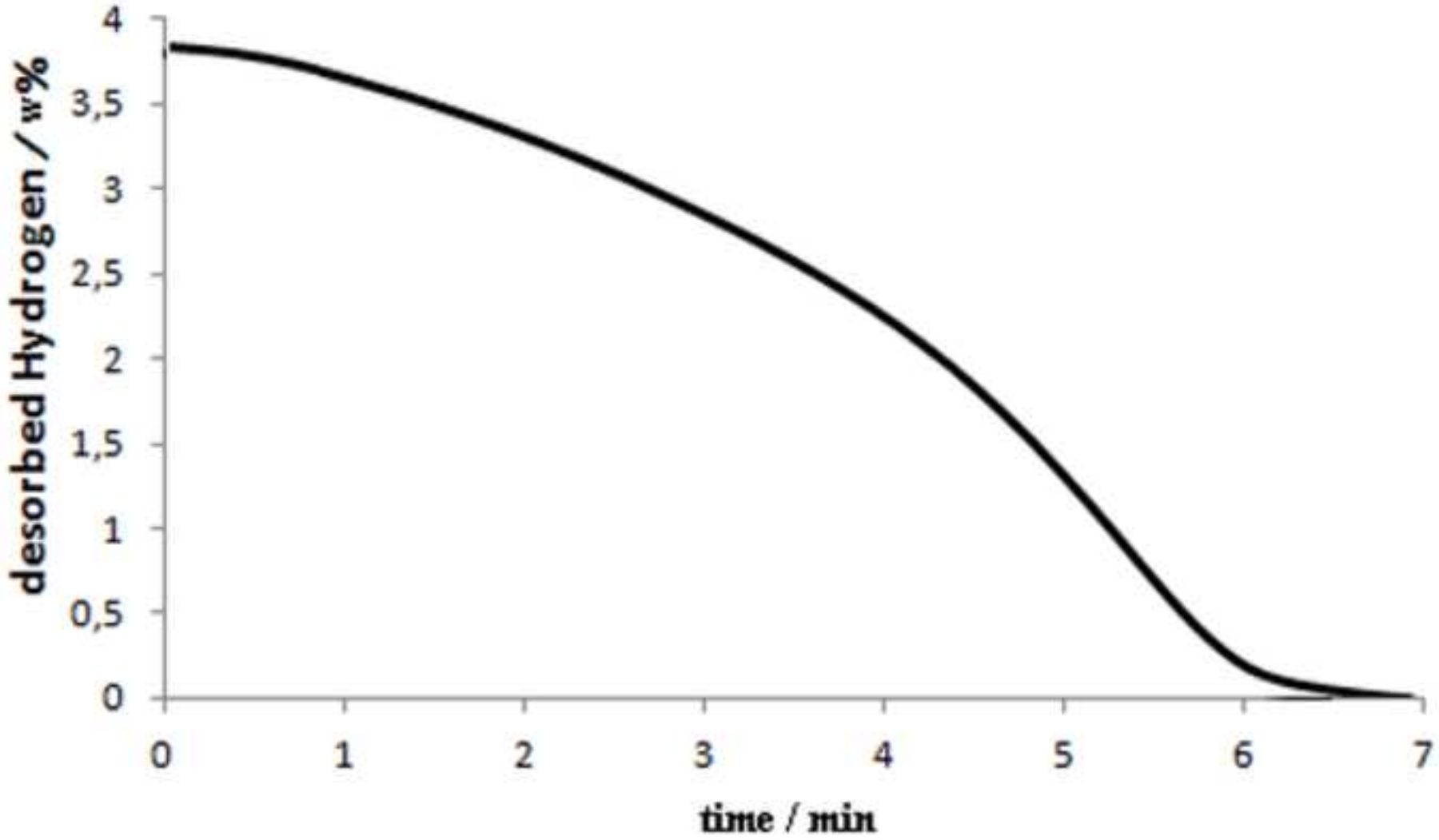

Figure 7

Click here to download high resolution image

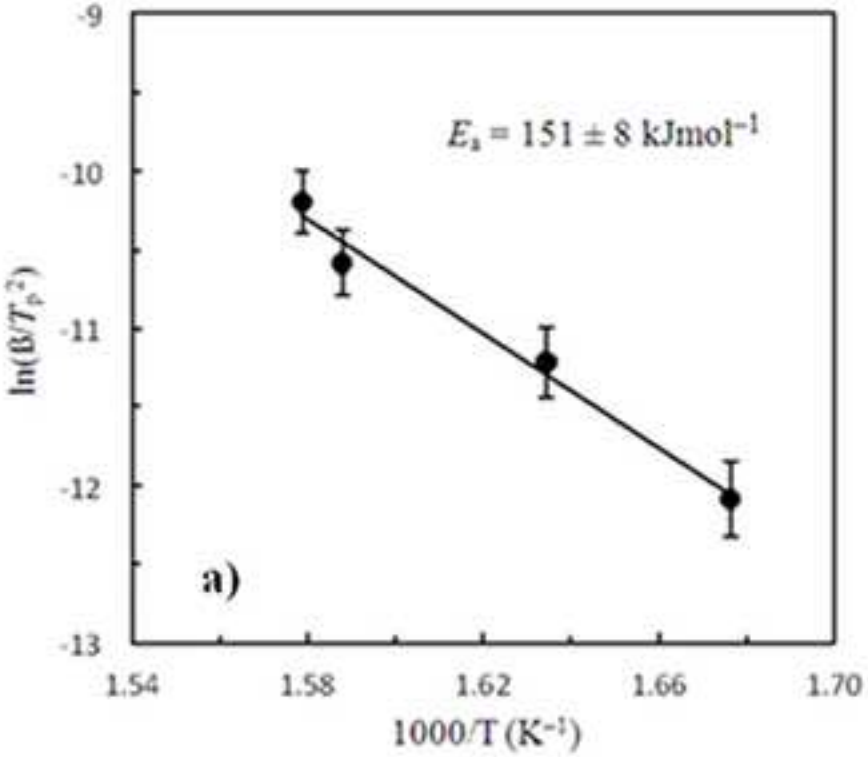

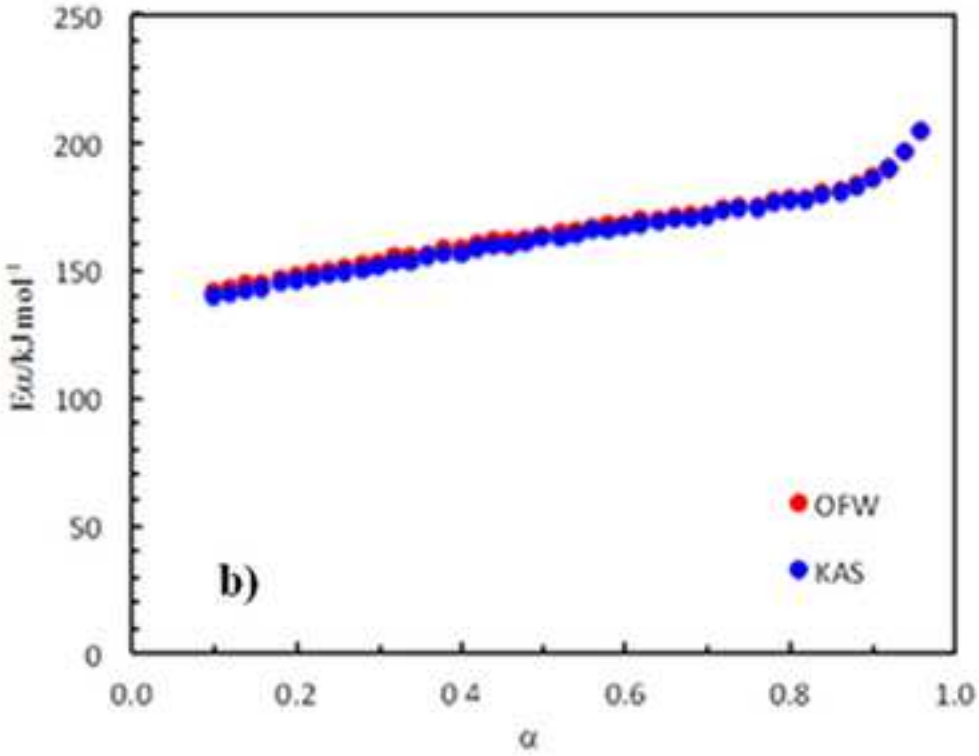

Figure 8

Click here to download high resolution image